

Equi-biaxial Flexural Fatigue Behavior of Thin Circular UHPFRC Slab-like Specimens

Xiujiang Shen & Eugen Brühwiler

Division of Maintenance and Safety of Structures (MCS-ENAC), Ecole Polytechnique Fédérale de Lausanne (EPFL), GC B2-402, Station 18, CH-1015 Lausanne, Switzerland

Abstract: This paper investigates experimentally the equi-biaxial flexural fatigue behavior of thin circular slab specimens made of Ultra High Performance Fibre Reinforced Cementitious Composite (UHPFRC), using ring-on-ring test method. The circular slab-like specimens represent an external tensile reinforcement layer for reinforced concrete (RC) slabs or a new thin slab element for the application, e.g. in bridge construction. Four series of flexural fatigue tests under constant amplitude fatigue cycles up to Very High Cycle Fatigue (20 million cycles) are conducted with varying stress levels S ranging from 0.47 to 0.76, targeting at the endurance limit of UHPFRC material and fatigue damage propagation under equi-biaxial stress condition. By means of digital image correlation (DIC) system, the tensile surface of each slab is monitored continually during testing, and the fatigue damage evolution is studied in terms of central deflection propagation. Based on the fatigue test results, a fatigue endurance limit is determined to be $S=0.50$, and four stages of fatigue damage evolution are characterized for the UHPFRC slabs with fatigue failure.

Keywords: biaxial flexural fatigue behavior, circular UHPFRC slab, ring-on-ring test method, digital image correlation (DIC), fatigue damage, Very High Cycle Fatigue

1. Introduction

Ultra-High Performance Fiber Reinforced Cementitious Composites (UHPFRC) are composed of a very compact cementitious matrix and a high amount of short and slender steel fibers. It possesses extremely low permeability, high ductility and high strength (compressive strength $\geq 180\text{MPa}$, tensile strength $\geq 10\text{MPa}$). A notable feature of UHPFRC subjected to uniaxial tension is the significant strain-hardening domain with 1%~5% of deformation capacity implying fiber activation and only smeared discontinuities in the bulk matrix before reaching the tensile strength. Furthermore, the fatigue endurance limit at multimillions-cycles exists in UHPFRC under uniaxial tensile or flexural loadings (Makita and Brühwiler, 2014a). These outstanding characteristics make UHPFRC fundamentally different from high performance concrete or fiber reinforced concrete, and suitable for the application on fatigue sensitive structural components (Brühwiler, 2018; Oosterlee, 2010).

Application of UHPFRC to specific zones of structural members under severe mechanical and environmental actions, such as bridge deck slabs, has been proven to be an effective method to improve (strengthen) structural members with respect to resistance and durability (Brühwiler, 2018; Denarié and Brühwiler, 2015). In the case of bridge deck slabs, the most fatigue loaded structural elements in bridges, the actual stress state caused by wheel loading is nearly equi-biaxial and far from uniaxial (Kim et al., 2015). And during the service duration, bridge decks are expected to be subjected to a high number of fatigue stress cycles, which may exceed 700 million (Rocha and Brühwiler, 2012).

Accordingly, this paper investigates experimentally the equi-biaxial flexural fatigue behavior of thin circular UHPFRC slab-like specimens, using the ring-on-ring test method. The

circular slabs represent an external tensile reinforcement layer for RC bridges or a new thin slab element as bridge deck. Four series of flexural fatigue tests under constant amplitude fatigue cycles up to 20 million cycles are conducted with varying S (stress level, the ratio of the maximum fatigue force to the load-carrying capacity of the slab), targeting at the endurance limit of UHPFRC and fatigue damage propagation under equi-biaxial stress condition.

2. Experimental Campaign

2.1 Test method

The ring-on-ring test method is applied for equi-biaxial flexural fatigue testing, using circular slab-like UHPFRC specimens with a diameter $R_0=600\text{mm}$ and a thickness $h=50\text{mm}$. Figure 1 shows the full test set-up and devices applied in this experimental campaign. The slab is simply supported on a steel support ring with $R=500\text{mm}$. Loading is imposed by a hydraulic jack acting on the center of slab through a steel force transmitting ring with $r=150\text{mm}$.

As illustrated in Figure 2, Digital Image Correlation (DIC) technique is applied to observe the full-field fatigue damage propagation during the whole fatigue testing process. In addition, two series of LVDT systems are installed on the top surface to measure the central deflection of slab and deformation of rubber pad, respectively. Further details about the ring-on-ring test applied in this study can be found in (Shen and Brühwiler, 2017).

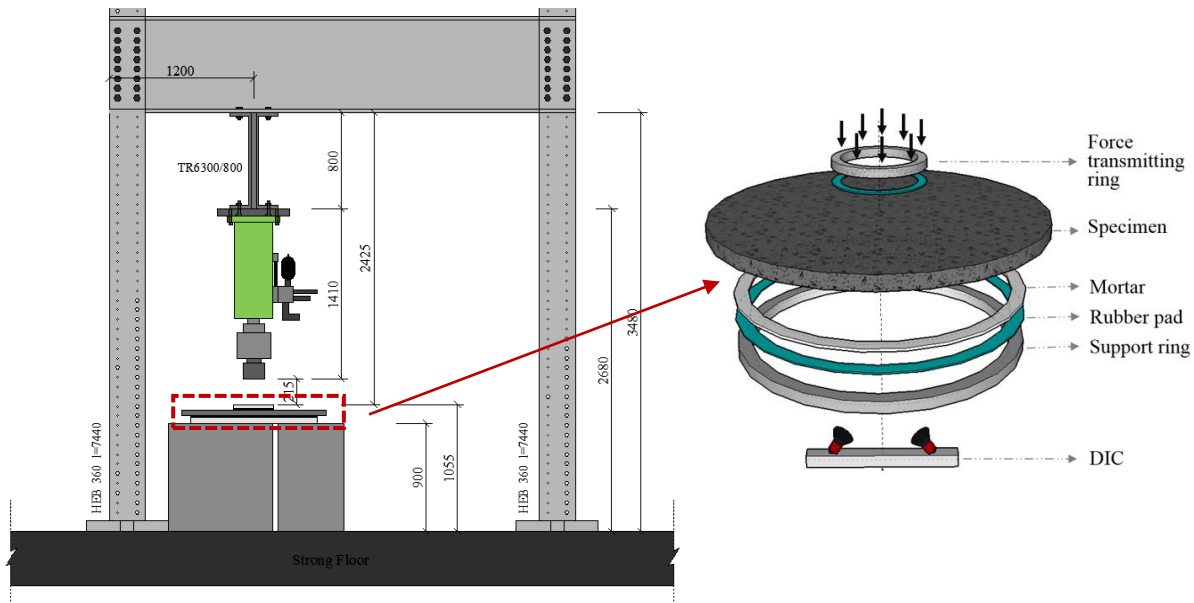


Figure 1. Schematic description of test setup

2.2 Material and specimen preparation

The chosen UHPFRC is an industrial premix containing 3.8% by volume of straight steel fibers with length of 13mm and diameter of 0.175mm, and its water/cement ratio is 0.15. The corresponding uniaxial tensile properties is shown in Table 1 (Shen and Brühwiler, 2018).

The circular slab-like specimens are cast in one step: the fresh mixture is poured in the center of the formworks, and let flow without any pulling or vibration. Once the casting was completed, a plastic sheet was pulled over the slabs to allow for auto-curing of the material. The slabs are demolded after 24 hours, then kept under moist curing conditions (20°C, 100% humidity) for the

following seven days; and subsequently, stored inside the laboratory until testing. The test age was more than 60 days, given that more than 90% of the UHPFRC material properties is attained after 60 days (Habel, 2004; Habel et al., 2006).

Table 1. Uniaxial tensile properties of UHPFRC

| E_U [GPa] | f_{Ute} [MPa] | f_{Utu} [MPa] | f_{Utu}/f_{Ute} | ε_{Ute} [%] | ε_{Utu} [%] | h [mm] |
|-------------|-----------------|-----------------|-------------------|-------------------------|-------------------------|----------|
| 49 | 8.26 | 10.10 | 1.24 | 0.18 | 2.39 | 50 |

2.3 Testing program

A total of sixteen slab-like specimens are prepared in the experimental campaigns: four quasi-static tests are carried out firstly for characterization of equi-biaxial flexural behavior of UHPFRC, and twelve fatigue tests with S ranging of 0.47~0.76 are performed with the aim to explore the fatigue endurance limit under equi-biaxial stress condition.

The fatigue testing procedure is quantitatively described in Figure 2. Firstly, all the slab-like specimens are subjected to three loading-unloading cycles up to 15kN with an actuator displacement rate of 1.0mm/min for loading preparation. Afterward, a monotonic loading with same displacement rate is applied up to the targeted maximum fatigue force $F_{fat,max}$ and unloaded to corresponding minimum fatigue force $F_{fat,min}$. This quasi-static loading-unloading part aims to predict the flexural resistance of each slab precisely. Then the sinusoidal cyclic loading with constant amplitude is imposed with frequency of 5Hz.

A smart DIC measurement program is applied during the fatigue tests as also illustrated in Figure 3. At the early age of fatigue loading, the DIC measurement is activated at every selected numbers of cycles with frequency of 50Hz.. Then the DIC measurement is activated at each 10'000th cycle during constant fatigue loading regime and at each 100th cycle during final unstable fatigue loading regime.

In this study, the values of $F_{fat,max}$ are actually varied between 47% and 76% of the average flexural resistance of the slab-like specimens, namely $S=0.47\sim 0.76$. The specific ratio R between $F_{fat,min}$ and $F_{fat,max}$ is arbitrarily chosen as 0.1. The fatigue endurance limit is defined as a force level below which no fatigue failure occurs up to 20 million cycles. With respect to bridge deck slabs, 20 million extreme force cycles are considered to be realistic to be reached during the service life for heavily trafficked bridges. Besides, the number of 20 million cycles is in the range of the VHCF domain (Makita and Brühwiler, 2014b; Sadananda et al., 2007).

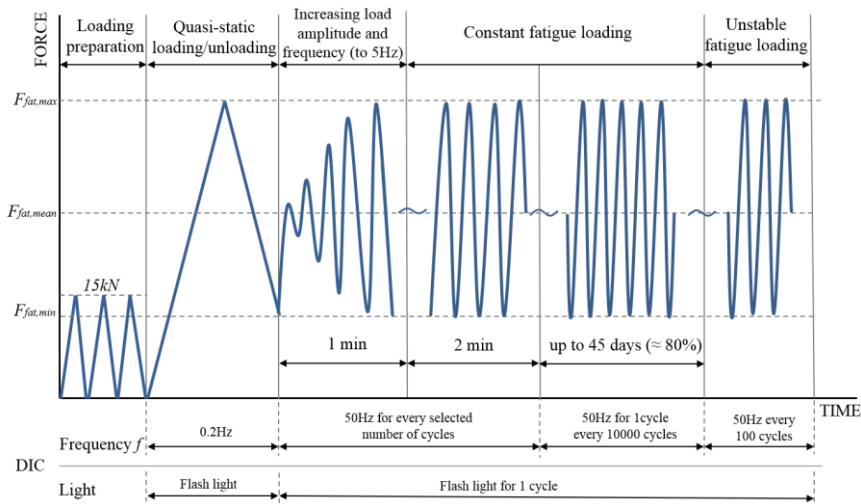


Figure 2. Qualitative fatigue loading history and DIC measurement program

3. Results and Analysis

3.1 Quasi-static flexural behavior of UHPFRC slab

The ring-on-ring test results of four UHPFRC slabs are presented in terms of force-deflection ($F-\delta$) curves of the central point (Figure 4). Accordingly, Table 4 summarizes the characteristic equi-biaxial flexural parameters for each slab, including the elastic limit force (F_{el}) and corresponding deflection (δ_{el}), peak force (F_p) and deflection (δ_p). The recorded force values are modified considering the real thickness of each slab by using the term $(h/h_i)^2$, where h is the nominal thickness (50 mm) and h_i is the measured thickness of each slab. Based on $F-\delta$ curves, the equi-biaxial response of UHPFRC slabs is discussed qualitatively by means of four characteristic phases marked with the letters A to D according to Figure 3:

(1) Elastic phase (Phase I, OA):

UHPFRC material provides a linear elastic response. Only a small part of the flexural resistance ($0.28F_p$), and very small portion of deflection is reached in this phase.

(2) Quasi-elastic phase (Phase II, AB):

In this phase, the tensile strain hardening UHPFRC is considered as a homogeneous material with smeared matrix discontinuities in the UHPFRC volume. It should be noted that a considerable portion of bending resistance develops with little loss of flexural stiffness, and the $F-\delta$ curves remains almost linear in this phase. Hereby, the end of this phase (point B) is defined as quasi-elastic limit, corresponding to $0.58F_p$ and $0.14\delta_p$ in average.

(3) Hardening phase (Phase III, BC):

Phase III is characterized by a gradual increase of UHPFRC material entering into the tensile softening regime, and consequentially, two levels of fictitious crack propagation. In the first roughly 70% of Phase III in terms of force-axis, the multiple fine fictitious cracks with small openings of less than 0.8mm and significant stress transfer develop. Thus, this first part contributes largely to the flexural resistance with minor increase of deflection in Phase III. For the rest of this phase, no new fictitious cracks appear. This second part undergoes significant deflection increase and only small resistance increase until F_p is reached. Conclusively, fictitious crack development in Phase III provides about 40% increase in flexural resistance and significant increase of deformations.

(4) Softening phase (Phase IV, CD):

Beyond F_p , the flexural response starts its softening behavior with continuous propagation of the dominant fictitious cracks. Deflection increases rapidly, while merely a slight decreasing in post-peak resistance is recorded, exhibiting pronounced post-peak behavior of the UHPFRC slab element.

Table 2. Characteristic biaxial flexural parameters of UHPFRC slabs

| No. | F_{el} (kN) | δ_{el} (mm) | F_p (kN) | δ_p (mm) | h (mm) | Thickness factor |
|-----------|------------------|-----------------------|---------------|--------------------|-------------|---------------------|
| S1-1 | 41.35 | 0.84 | 138.66 | 31.75 | 50.30 | 0.99 |
| S1-2 | 39.11 | 0.78 | 142.64 | 19.06 | 51.81 | 0.93 |
| S1-3 | 39.87 | 0.72 | 144.38 | 25.01 | 50.48 | 0.98 |
| S1-4 | 42.01 | 0.72 | 135.14 | 29.46 | 46.43 | 1.16 |
| Average | 40.59 | 0.77 | 140.21 | 26.32 | - | - |
| Std. dev. | 1.33 | 0.06 | 4.14 | 5.59 | - | - |
| CV | 0.03 | 0.08 | 0.03 | 0.21 | - | - |

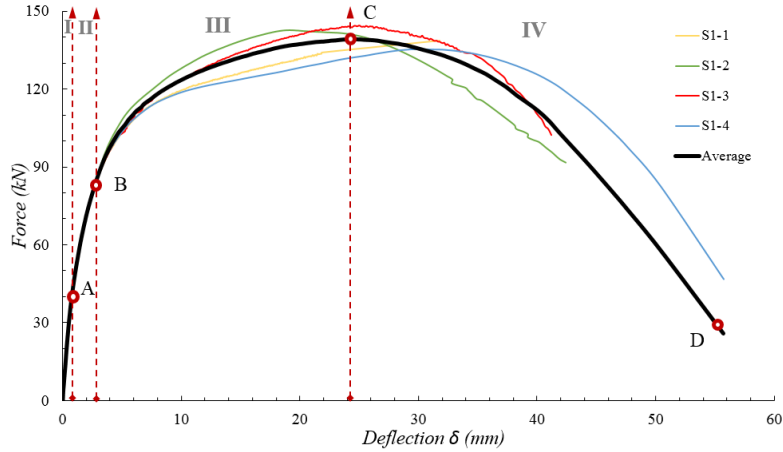


Figure 3. Force-deflection response of four UHPFRC circular slabs

3.2 Flexural fatigue behavior of UHPFRC slab

3.2.1 Fatigue life and S-N curves

The results of flexural fatigue tests on UHPFRC slab-like specimens are summarized in Table 3, where data from nine slabs are given. It should be noted that the ultimate flexural resistance $F_{p,pre}$ of each slab was predicted based on the measured thickness h . Also, the fatigue results are presented in an S-N diagram (Wöhler diagram), as shown in Figure 4.

From the overall test results, the fatigue endurance limit of UHPFRC slab-like specimens under equi-biaxial stress condition is estimated to be at an S-level of roughly 0.50, as indicated by the dashed line in Figure 4. Above this limit, significant damage leading to rather short fatigue life is observed. Based on the previous quasi-static test results (section 3.1), $S=0.50$ is in the final part of the quasi-elastic domain of flexural response, where large part of matrix discontinuities (strain-hardening) is developed in UHPFRC material. Thus, it can be deduced that the matrix discontinuities don't lead to detrimental damage of UHPFRC under flexural fatigue loading.

According to Figure 5, the following linear relation between S and $\log(N_f)$ is determined without considering run-outs:

$$S = -0.1255 \log(N_f) + 1.2556 \quad (1)$$

The accuracy of the prediction is represented by a correlation coefficient of $R^2=0.87$, indicating a good dependency between the two variables. This can owe to the reliable prediction of each slab's flexural resistance, as also found by C. Loraux (Loraux, 2018).

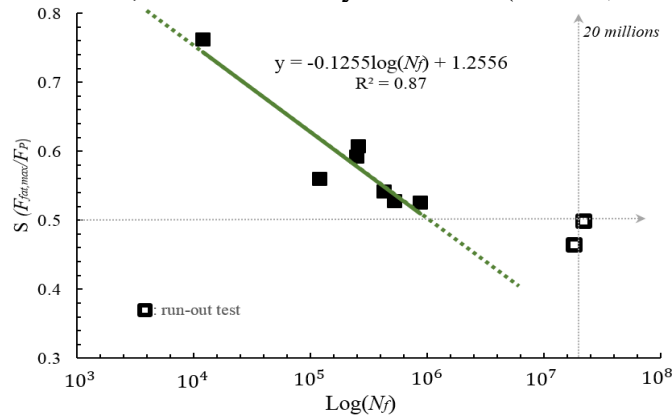


Figure 4. S-N diagrams

Table 3. Results of flexural fatigue tests

| Specimen | h (mm) | $F_{P,pre}$ (kN) | $F_{fat,max}$ (kN) | $F_{fat,min}$ (kN) | S | N_f (million) | Remarks |
|----------|-------------|---------------------|-----------------------|-----------------------|------|--------------------|---------|
| F-S1-1 | 48.40 | 131.38 | 100.00 | 10.00 | 0.76 | 0.01 | - |
| F-S1-2 | 51.70 | 149.91 | 91.00 | 10.00 | 0.61 | 0.26 | - |
| F-S1-3 | 49.80 | 139.09 | 83.00 | 7.30 | 0.60 | 1.60 | - |
| F-S1-4 | 54.36 | 165.73 | 98.00 | 8.00 | 0.59 | 0.25 | - |
| F-S1-5 | 55.89 | 175.19 | 98.00 | 10.00 | 0.56 | 0.12 | - |
| F-S1-6 | 50.36 | 142.24 | 77.00 | 7.00 | 0.54 | 0.43 | - |
| F-S1-7 | 54.49 | 166.52 | 87.50 | 7.00 | 0.53 | 0.88 | - |
| F-S1-9 | 52.11 | 152.29 | 76.00 | 10.00 | 0.50 | 21.90 | run-out |
| F-S1-8 | 51.81 | 150.52 | 70.00 | 7.00 | 0.47 | 18.00 | run-out |

3.2.2 Fatigue failure mode

The representative cracking patterns (visible by the naked eye) on the bottom surface after testing at various force levels ($S=1.0, 0.60, 0.54$ and 0.47) are illustrated in Figure 5, where the black thick lines refer to the dominant fictitious cracks or real cracks, and the thin ones stand for fine fictitious cracks. Similarly, all slabs failed in flexural fracture mode, characterized by several random dominant fictitious cracks or real cracks concentrated within the area under the force transmitting ring in the center of slabs. Under quasi-static loading ($S=1.0$), significant multiple fine fictitious cracks with uniform distribution are highlighted in the slab; while fewer fine fictitious cracks are observed for slabs under fatigue loading. It is noted that the number of fine fictitious cracks in slabs under fatigue decreases with decreasing S level. In particular, only a few fine fictitious cracks are observed in slabs with S close to or below the fatigue endurance limit (i.e., $S=0.54$ or 0.47). Similar phenomenon is also found in the direct tensile and flexural fatigue behavior (Huang et al., 2018; Suthiwarapirak et al., 2004).

Based on previous quasi-static test (section 3.1), the multiple fine fictitious cracks behavior contributes largely to the resistance and rigidity in the hardening domain of the flexural response. In practice, bridge structures are generally under traffic fatigue loading with relatively low stress levels. This means that the hardening characteristics of the UHPFRC slab become less pronounced in this case. This phenomenon is noticeable for future application of this material.

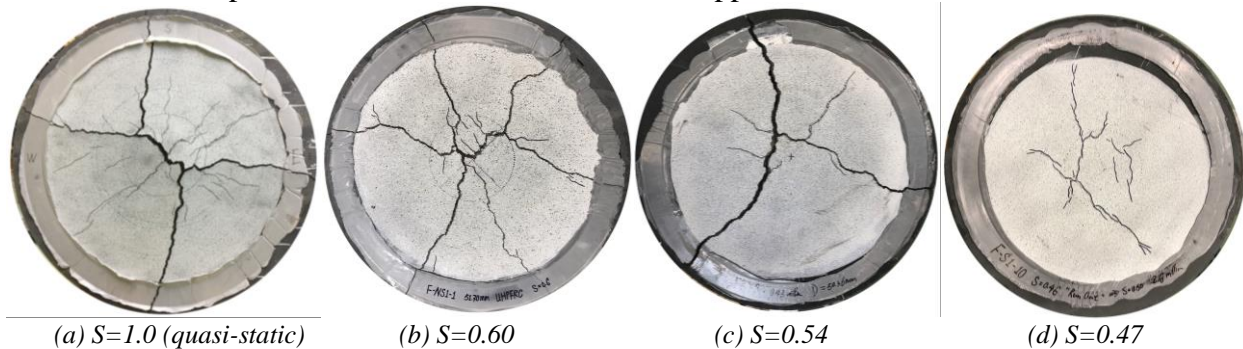


Figure 5. Typical cracking patterns of slabs after testing at various force levels

3.2.3 Fatigue damage evolution

The damage evolution of UHPFRC slabs under flexural fatigue loading is discussed in terms of central deflection as measured by both LVDT and DIC systems. The evolution of central deflection

is presented here with the increase of normalized fatigue cycles N/N_f , and the corresponding data were the maximum and minimum deflection at each fatigue loading cycle. Although only two typical evolution diagrams are illustrated here (i.e., one for slab with fatigue failure and one for run-out), other diagrams show similar phenomena.

Regarding the UHPFRC slabs with fatigue failure, the evolution of the central deflection under flexural fatigue loading is generally S-shaped, as illustrated in Figure 6(a). The evolution curves can be characterized by four distinct stages with respect to the deflection propagation rate, which is different from the three-stage curve of concrete. The stage I is the rapid propagation phase. The stage II and III are the constant propagation stages with different increasing rates. The increasing rate in stage III is distinctly higher than that in stage II. It is noted that stage II and III occupy roughly 50% and 20% of the slab's fatigue life. In the final unstable stage (IV), a significant deflection propagation with increasing rate is observed.

With respect to the UHPFRC slabs with run-out, only three stages are distinguished in the deflection evolution diagrams (Figure 6-b). Stage I is the rapid propagation domain, similar to that of slabs with fatigue failure. Stage II refers to the stable propagation domain with lower increasing rate compared with that from the slabs with fatigue failure. Afterwards, no further deflection propagation is observed (stage III).

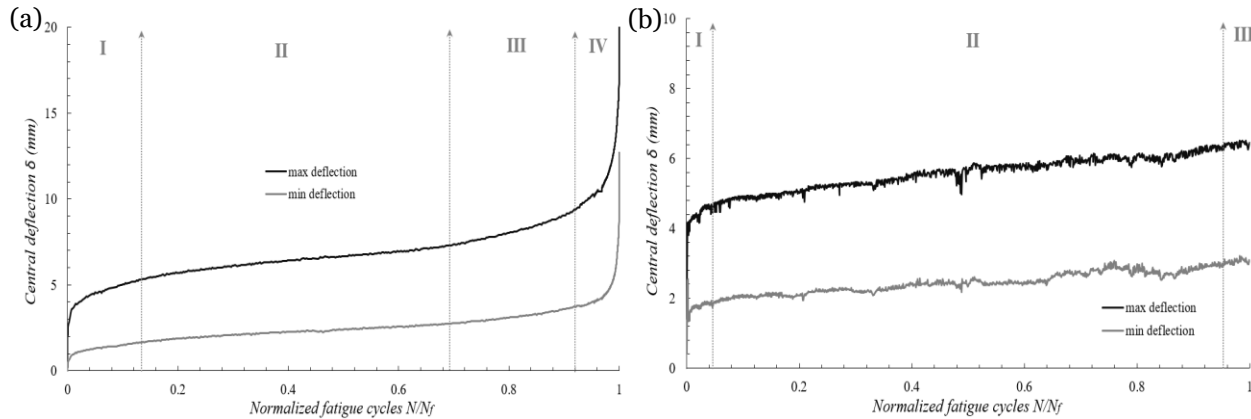


Figure 6. Evolution curve of central deflection under flexural fatigue loading
(a) $S=0.53$, $N_f=0.88$ million, (b) $S=0.50$, run-out

4. Conclusions

In this study, the flexural fatigue behavior of UHPFRC circular slab specimens with various stress levels under equi-biaxial stress state is investigated using the ring-on-ring test method. The main conclusions are:

- A constant amplitude fatigue endurance limit at VHCF (20 million cycles in this study) is determined to be at a solicitation level $S=0.50$ for UHPFRC slab-like specimen under equi-biaxial flexural stress state. This suggests that the matrix discontinuities in UHPFRC do not lead the detrimental fatigue damage under equi-biaxial stress state.
- The multiple fine fictitious cracks behavior of UHPFRC slab becomes less pronounced with decrease of S levels (as increase of fatigue cycles) under equi-biaxial stress state. In particular, only a few fine fictitious cracks are observed for the run-out slabs.
- Four stages of fatigue damage evolution are characterized for UHPFRC slab-like specimens with fatigue failure, while there were only three stages for the run-out slabs.

5. References

- Brühwiler, E., 2018. “Structural UHPFRC” to enhance bridges, in: Keynote Lecture, 2nd International Conference on UHPC Materials and Structures (UHPC 2018 - China). Fuzhou, China, pp. 140–158.
- E. Denarié, E. Brühwiler, Cast-on site UHPFRC for improvement of existing structures—achievements over the last 10 years in practice and research, in: 7th Workshop on High Performance Fiber Reinforced Cement Composites, 1-3, June 2015, Stuttgart, Germany, 2015.
- K. Habel, Structural behaviour of elements combining ultra-high performance fibre reinforced concretes (UHPFRC) and reinforced concrete, Doctoral Thesis (EPFL). (2004).
- K. Habel, M. Viviani, E. Denarié, E. Brühwiler, Development of the mechanical properties of an Ultra-High Performance Fiber Reinforced Concrete (UHPFRC), *Cement and Concrete Research*. 36 (2006) 1362–1370.
- Huang, B.-T., Li, Q.-H., Xu, S.-L., Zhou, B.-M., 2018. Tensile fatigue behavior of fiber-reinforced cementitious material with high ductility: Experimental study and novel P-S-N model. *Constr. Build. Mater.* 178, 349–359.
- Kim, J., Kim, D.J., Park, S.H., Zi, G., 2015. Investigating the flexural resistance of fiber reinforced cementitious composites under biaxial condition. *Compos. Struct.* 122, 198–208.
- Loroux, C.T., 2018. Long-term monitoring of existing wind turbine towers and fatigue performance of UHPFRC under compressive stresses (doctoral thesis, 8404). École polytechnique fédérale de Lausanne (EPFL).
- T. Makita, E. Brühwiler, Tensile fatigue behaviour of ultra-high performance fibre reinforced concrete (UHPFRC), *Mater Struct.* 47 (2014) 475–491.
- Makita, T., Brühwiler, E., 2014b. Tensile fatigue behaviour of Ultra-High Performance Fibre Reinforced Concrete combined with steel rebars (R-UHPFRC). *Int. J. Fatigue* 59, 145–152.
- Oesterlee, C., 2010. Structural response of reinforced UHPFRC and RC composite members (doctoral thesis, 4848). École polytechnique fédérale de Lausanne (EPFL).
- M. Rocha, E. Brühwiler, Prediction of fatigue life of reinforced concrete bridges using Fracture Mechanics, in: *Proceedings Bridge Maintenance, Safety, Management, Resilience and Sustainability*, CRC Press/Balkema, 2012: pp. 3755–3761.
- K. Sadananda, A.K. Vasudevan, N. Phan, Analysis of endurance limits under very high cycle fatigue using a unified damage approach, *International Journal of Fatigue*. 29 (2007) 2060–2071.
- Shen, X., Brühwiler, E., 2017. Flexural quasi-static behavior of UHPFRC circular slab specimens. *AFGC-ACI-Fib-RILEM Int Symp. Ultra-High Perform. Fibre-Reinf. Concr. UHPFRC 2017*.
- Shen, X., Brühwiler, E. 2018. Characterization of Tensile Behavior in UHPFRC Thin Slab Using NDT Method and DIC System, in: *Proceedings PRO 129*. Presented at the 2nd International Conference on Ultra High Performance Concrete Materials and Structures, UHPC 2018, Fuzhou, China.
- Suthiwarapirak, P., Matsumoto, T., Kanda, T., 2004. Multiple cracking and fiber bridging characteristics of engineered cementitious composites under fatigue flexure. *J. Mater. Civ. Eng.* 16, 433–443.